Vaccine 27 (2009) 3953–3962

Contents lists available at ScienceDirect

Vaccine

journal homepage: www.elsevier.com/locate/vaccine

Identification of conserved erythrocyte binding regions in members of the *Plasmodium falciparum* Cys_6 lipid raft-associated protein family

Jeison García[a,b], Hernando Curtidor[a,b], Carlos G. Pinzón[a,b], Magnolia Vanegas[a,b], Armando Moreno[a,b], Manuel E. Patarroyo[a,c,*]

[a] *Fundación Instituto de Inmunología de Colombia FIDIC, Carrera 50 No. 26-20, Bogotá, Colombia*
[b] *Universidad del Rosario, Calle 14 No. 6-25, Bogotá, Colombia*
[c] *Universidad Nacional de Colombia, Carrera 45 No. 26-85, Bogotá, Colombia*

ARTICLE INFO

Article history:
Received 6 February 2009
Received in revised form 3 April 2009
Accepted 15 April 2009
Available online 3 May 2009

Keywords:
Antimalarial vaccine
Cys_6 family
High-activity binding peptides
*Pf*12
*Pf*38
*Pf*41
Plasmodium falciparum

ABSTRACT

Detergent-resistant lipid raft membrane-associated *Pf*12, *Pf*38 and *Pf*41 proteins belong to the Cys_6 family, whose members are implicated in *Plasmodium falciparum* invasion to erythrocytes. We have analyzed the interaction between 20-mer-long synthetic peptides spanning the entire *Pf*12, *Pf*38 and *Pf*41 sequences and erythrocytes. Eight high-activity binding peptides (HABPs) were identified in these proteins, which presented saturable bindings susceptible to erythrocytes' enzymatic treatment, and β-turn, random coil and α-helical elements as principal structural features. Some of these HABPs inhibited merozoite invasion *in vitro*, suggesting a possible role of *Pf*12, *Pf*38 and *Pf*41 during erythrocyte invasion and supporting their inclusion in the design of a fully effective antimalarial vaccine.

1. Introduction

Several studies have been conducted in the search for a completely effective vaccine against malaria, a parasitic disease caused in humans by four *Plasmodium* species; being *Plasmodium falciparum* the most lethal one as it accounts for 500 million cases and more than 3 million annual deaths around the world [1]. During the *P. falciparum* parasite's life cycle, merozoites invade erythrocytes through a wide range of specific molecular interactions between merozoite proteins and erythrocyte surface receptors [2]. Once inside erythrocytes, merozoites develop and undergo several division cycles that end up with the production of new merozoites that go on to infect other erythrocytes, being this the stage responsible for the main symptoms associated to this disease.

Several merozoite membrane proteins have been implicated in the initial contact between merozoites and erythrocytes, which results in the formation of an irreversible junction once apical organelles have released their contents [2–4]. These studies highlight the importance of apical organelle-associated proteins (contained inside micronemes, rhoptries and dense granules) as well as of parasite's surface molecules as potential candidates for the design of new vaccines against malaria [2,3].

Among merozoite proteins involved in erythrocyte invasion, a set of surface proteins expressed both by asexual (merozoites) and sexual stages (gametocytes) have been widely studied [5–8]. These molecules have been grouped within the multi-stage Cys_6 protein family based on the presence of six notably conserved cysteine residues forming structurally similar domains in these proteins [5] (Fig. 1a and b).

The release of the *P. falciparum* genome has enabled the identification of a group of 10 proteins sharing the abovementioned structural feature [5,9,10], most of which are expressed by parasite sexual stages. Among these proteins, *Pfs*230p, *Pfs*230 and *Pfs*48/45 are expressed on the surface of gametocytes (where the two latter proteins form a complex), whereas other proteins such as *Pfs*47 are only expressed by female gametes [11]. Additionally, the *P. berghei* homolog to *Pf*36 identified on sporozoite surface has been also implicated as an important protein for hepatocyte invasion [12], while two recently described merozoite membrane-associated proteins, named *Pf*92 and *Pf*113, have been detected in detergent-resistant membrane domains (DRMs) anchored via glycosyl-phosphatidyl-inositol (GPI) motifs. All these findings highlight Cys_6 family members as excellent antimalarial vaccine candidates [13].

* Corresponding author at: Fundación Instituto de Inmunología de Colombia, Carrera 50 No. 26-20, Bogotá, Colombia. Tel.: +57 1 4815219; fax: +57 1 4815269.
E-mail address: mepatarr@mail.com (M.E. Patarroyo).

0264-410X/$ – see front matter © 2009 Elsevier Ltd. All rights reserved.
doi:10.1016/j.vaccine.2009.04.039

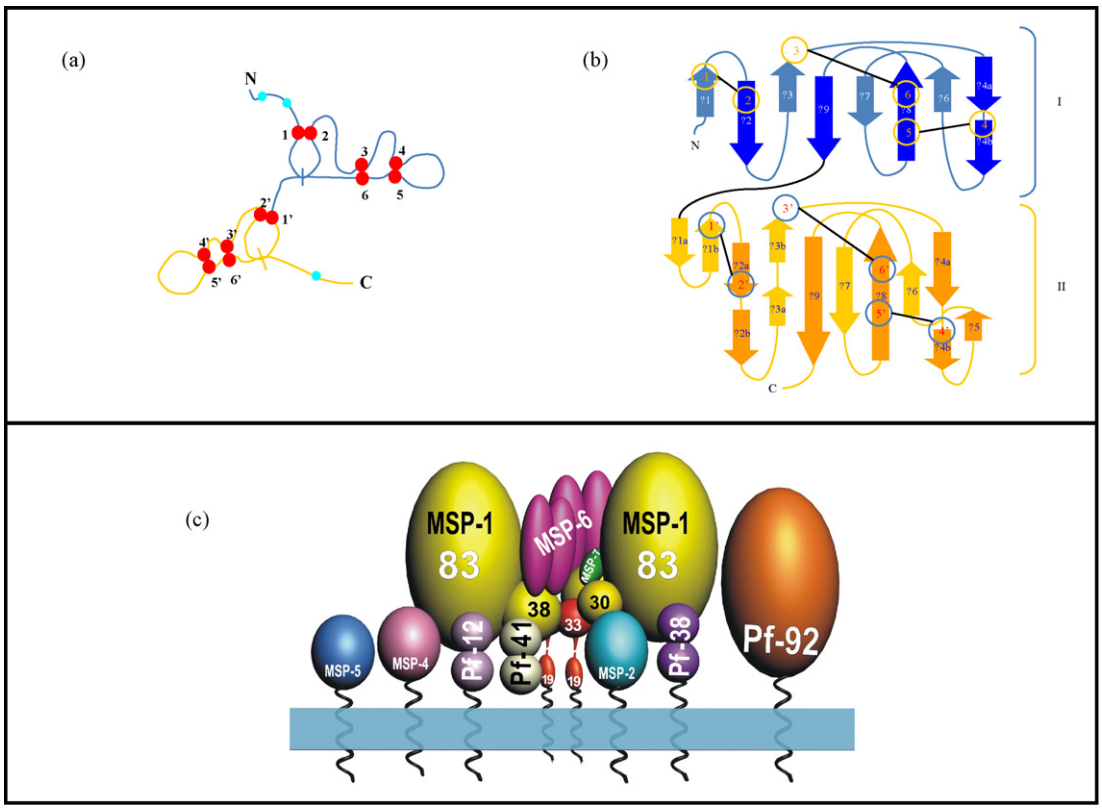

Fig. 1. Structural models of sexual stage *Plasmodium falciparum* Cys_6 family proteins and of their localization in detergent-resistant membranes. (a) Schematic representation of the *Pf*12 protein. The six representative cysteine residues forming disulfide bonds in domain I (blue ribbon) and II (orange ribbon) are marked by red circles, while light-blue circles represent unpaired cysteine residues. (b) Structural representation of *Pf*12, β-strands in domains I and II are indicated by blue arrows and orange arrows, respectively. (c) Scale diagram showing DRM-associated proteins found in *P. falciparum* merozoite membrane lipid rafts domains where *Pf*12 (violet), *Pf*38 (dark violet) and *Pf*41 (gray) are located. The diagram also shows molecules (MSP-1, -2, -4, -5 and *Pf*92) anchor via GPI-tail (depicted as black twists), and some non-covalently associated proteins ($MSP\text{-}1_{19}$, $MSP\text{-}1_{30}$, $MSP\text{-}1_{38}$, $MSP\text{-}1_{83}$, $MSP\text{-}6_{36}$ and MSP-7). Figures were adapted from Pinzon et al. (Fig. 1c) [18] and Gerloff et al. (Fig. 1a and b) [5].

Three Cys_6 proteins are expressed by *P. falciparum* asexual stages, named *Pf*12, *Pf*38 and *Pf*41. Of these proteins, *Pf*12 (39.4 kDa) anchors to merozoite membrane via a GPI motif, same as several other merozoite adhesins such as merozoite surface proteins (MSPs), which have been recognized as important antimalarial vaccine targets and are involved in the formation of raft-like lipid domains or detergent-resistant membrane-associated macromolecular complexes involved in numerous cellular signaling and recognition events [5,13–15]. Previous studies have used *Pf*12 as the structural prototype for studying Cys_6 proteins due to the presence of two prominent Cys-rich domains (Fig. 1a and b): domain I, which is defined by three disulfide bridges formed between Cys 31–53, Cys 67–138 and Cys 81–136; and domain II that also contains three disulfide bridges formed between Cys 179–211, 225–286, and 236–284 [5].

*Pf*38 is a 40.6 kDa GPI-anchored merozoite membrane protein that is expressed in both sexual and asexual stages [8,13,14]. The third Cys_6 asexual protein, *Pf*41 (43.1 kDa), has been located on merozoite surface where it interacts with other GPI-anchored merozoite membrane proteins via non-covalent interactions given the lack of a GPI-anchoring motif in its sequence (Fig. 1c) [5,13].

*Pf*12, *Pf*38 and *Pf*41 have been found to form part of DRM complexes, suggesting the possible role of these proteins as ligands during merozoite invasion of erythrocytes (Fig. 1c). Additionally, the strong recognition of these proteins by sera from naturally infected patients indicates that they are exposed to the immune system's attack [13]; although a precise role in parasite binding to host cells has not been described for these proteins to date. Due to all the aforementioned evidence, these three proteins are considered attractive candidates for vaccine development studies.

With the aim of elucidating the specific role played by these three Cys_6 proteins in merozoite invasion, we have finely mapped their sequences through the use of synthetic peptides, following a robust and highly specific receptor–ligand assay developed at our Institute as an important tool in the development of a logical and rational vaccine design methodology [16]. This methodology has enabled the identification of peptide sequences binding with high specificity and activity to *P. falciparum* host cells (namely high-activity binding peptides or HABPs), in several parasite proteins implicated in erythrocyte invasion [17–20].

We have previously demonstrated that conserved non-immunogenic HABPs identified on parasite invasion-associated proteins such as $MSP\text{-}1_{19}$ [21], the erythrocyte binding antigen 175 (EBA-175) [22], the apical membrane antigen 1 (AMA-1) [23] and the thrombospondin-related anonymous protein (TRAP) [24] maintain the same structure they display in their corresponding native proteins [25–28]. Moreover, some HABPs have been implicated in parasite invasion to host cells, such as EBA-175 HABP 1783 [22], which is located inside EBA-175 region II and has been directly implicated in erythrocyte binding and EBA-175 dimerization [26]. The TRAP HABP 3287/3289 [24,29] has been also located in a heparin-binding site recently described for this protein [25]. All these results support the use of synthetic peptides in the identification of binding regions of *P. falciparum* proteins.

This work describes the fine mapping of *Pf*12, *Pf*38 and *Pf*41 protein regions binding specifically to human erythrocytes. The localization of these HABPs inside structurally similar regions suggests the presence of a possibly conserved binding domain in Cys_6 proteins. Once *Pf*12, *Pf*38 and *Pf*41 HABPs were identified, their bindings to erythrocytes were partially characterized in enzymatic

treatment and cross-linking assays, and the possible biological role of these HABPs in erythrocyte invasion was assessed *in vitro* by performing invasion inhibition assays with *P. falciparum* merozoites (FBC-2 strain). The results indicate the participation of Cys_6 proteins in merozoite invasion to erythrocytes and support the inclusion of their HABPs as potential components of a fully effective, multistage, subunit-based, chemically produced antimalarial vaccine, once their amino acid sequences have been properly modified by altering their spatial configuration so they can fit properly into Class II Major Histocompatibility Complex molecules (MHC-II) and hence induce a protective immune response against *P. falciparum* challenge in the *Aotus* monkey model [16,23,30–32].

2. Materials and methods

2.1. Pf12, Pf38 and Pf41 peptides synthesis

The solid phase peptide synthesis methodology was employed for synthesizing 20-residue-long peptides covering the complete sequence of the *P. falciparum* 3D7 strain *Pf*12 (**PFF0615c**), *Pf*38 (**PFE0395c**) and *Pf*41 (**PFD0240c**) proteins [33]; using *t*-Boc protected amino acids (Bachem) and a 0.7 mEq/g 4-methylbenzhydrylamine hydrochloride (MBHA) resin [34,35]. Synthesized peptides were cleaved by low-high HF techniques, [36] purified by RP-HPLC and analyzed by MALDI-ToF mass spectroscopy. A tyrosine residue was added to the C-terminus region of peptides not containing such residue in their sequence to allow radiolabeling. All peptides were numbered according to our institute's serial system (Fig. 2).

2.2. ^{125}I radiolabeling of peptides

Radiolabeling of synthetic peptides was performed according to previously described methodologies [20,37]. Briefly, 5 μL of each synthesized peptide (1 mg/mL) were dissolved in HBS buffer (0.01 M HEPES, 0.15 M NaCl, pH 7.4) and then radiolabeled with a 5 μL $Na^{125}I$ (MP Biomedicals, 100 mCi/mL) and 15 μL of 13.5 μM chloramine-T solution. Once 15 min had elapsed, the reaction was stopped with 15 μL of 14 μM $NaHSO_3$. The ^{125}I-peptides were then purified by size exclusion chromatography in a Sephadex G-10 column (Pharmacia) using HBS buffer as mobile phase, before measuring their radioactivity in a gamma counter (Auto Gamma Counter Cobra II, Packard).

2.3. Erythrocyte binding assays

Leukocyte-free erythrocyte suspensions containing 1×10^8 cells obtained from healthy donors were incubated for 60 min with increasing concentrations of ^{125}I-labeled peptide (0–560 nM) in the absence (total binding) or presence of unlabeled peptide (nonspecific binding) in triplicate. Erythrocytes were then washed twice with HBS isotonic buffer and the amount of bound radiolabeled peptide was measured in a gamma counter [18–20]. A peptide was considered to be a high-activity binding peptide whenever it presented ≥2% specific binding activity, defined as the slope of the specific binding curve (specific binding = total binding − nonspecific binding) between the amount of radiolabeled peptide bound specifically to erythrocytes and added radiolabeled peptide at four different logarithmic concentrations, according to a previously established criteria [19,20,32] (Fig. 2a–c). Once HABPs were identified, scrambled peptides having the same amino acid composition but different sequence were synthesized and their binding activities were also determined by following the same methodology (Fig. 2d).

2.4. HABPs saturation assays

The kinetic constants of each HABP were determined by incubating 7.5×10^7 erythrocytes with increasing concentrations of radiolabeled peptide (0–2200 nM) in the absence or presence of unlabeled peptide (2.4×10^4 nM). Cells were then washed twice with HBS and the associated radioactivity was measured using a gamma counter [17,38,39]. All peptides were tested in triplicate same as in erythrocyte binding assays.

2.5. Effect of enzymatic treatment on HABP–erythrocyte binding

Membranes of human erythrocytes were modified by enzymatically treating cells with neuraminidase (150 μU/mL), chymotrypsin (1 mg/mL) or trypsin (1 mg/mL) according to a previously established protocol [17]. Briefly, erythrocyte suspensions (60% hematocrit) were independently incubated with each enzyme for 1 h at 37 °C. Cells were then washed and diluted to 20% hematocrit. Binding assays were then carried out as described above (in triplicate) in order to determine specific binding between HABPs and enzyme-treated erythrocytes, using HABPs' binding to untreated erythrocytes as binding control (100% binding).

2.6. Cross-linking assays

A total of 2.1×10^7 erythrocytes obtained from regular binding assays with radiolabeled HABPs were cross-linked using 50 μL bis(sulfosuccinimidyl)-suberate (BS^3, 1 mg/mL; Pierce) for 1 h at 4 °C. The reaction was stopped by adding Tris–HCl buffer and cross-linked HABPs were washed with hypotonic HBS before separating disrupted cell membranes by centrifugation. Membranes were collected in a 15 μL lysis cocktail (5 mM Tris–HCl buffer, 7 mM NaCl, 1 mM EDTA and 0.1 mM phenyl methyl sulfonyl fluoride (PMSF)), diluted in 15 μL Laemmli buffer and then centrifuged at $15{,}000 \times g$ for 15 min. Extracted proteins were separated by 12% SDS-PAGE using pre-stained protein molecular weight markers (MWM) (New England Bio Labs) and then analyzed using the BioRad molecular imager FX system [18].

2.7. Invasion inhibition assays with Pf12, Pf38 and Pf41 HABPs

HABPs were tested for their ability to inhibit *P. falciparum* merozoite invasion to erythrocytes *in vitro* by using schizont-synchronized intra-erythrocytic parasite cultures [40] seeded in 96-well plates in the presence of each HABP (200 μM). Following incubation at 37 °C for 18 h in an inert 5% O_2, 5% CO_2 and 90% N_2 atmosphere, culture supernatants were harvested and cells were washed with PBS for hydroethidine labeling. Once 30 min had elapsed, cells were washed at 37 °C and the suspension was analyzed using a FacsCalibur flow cytometer (FACsort, FL2 channel). These assays were done in triplicate, taking EGTA- and chloroquine-treated infected erythrocytes as inhibition controls and healthy erythrocytes as the invasion control [41].

2.8. Circular dichroism analysis

The secondary structure folding of each HABP was assessed by analyzing their circular dichroism spectra. Peptides at a 5 μM concentration were analyzed in 30% (v/v) TFE aqueous solution, using a 1-cm optical-length quartz cell thermostated at 20 °C. Spectra were acquired in a Jasco J-810 (JASCO Inc.) equipment by averaging three sweeps taken at 20 nm/min. Data were processed using the Spectra Manager software [42,43] and analyzed using SELCON, CONTINLL and CDSSTR deconvolution programs [44].

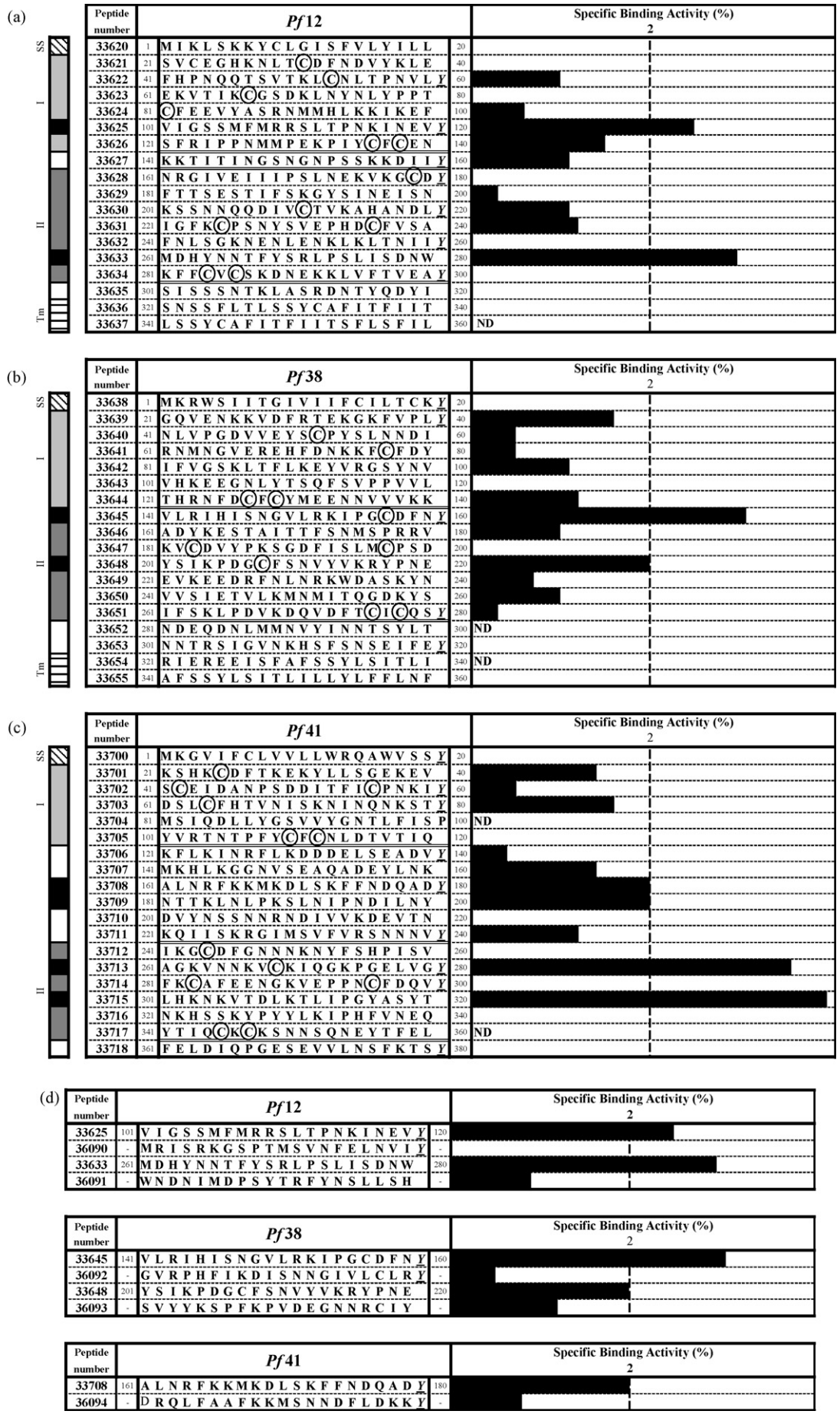
(a)
Peptide number
Pf12
Specific Binding Activity (%)
2
SS
I
II
Tm
33620 1 M I K L S K K Y C L G I S F V L Y I L L 20
33621 21 S V C E G H K N L T C D F N D V Y K L E 40
33622 41 F H P N Q Q T S V T K L C N L T P N V L Y 60
33623 61 E K V T I K C G S D K L N Y N L Y P P T 80
33624 81 C F E E V Y A S R N M M H L K K I K E F 100
33625 101 V I G S S M F M R R S L T P N K I N E V Y 120
33626 121 S F R I P P N M M P E K P I Y C F C E N 140
33627 141 K K T I T I N G S N G N P S S K K D I I Y 160
33628 161 N R G I V E I I I P S L N E K V K G C D Y 180
33629 181 F T T S E S T I F S K G Y S I N E I S N 200
33630 201 K S S N N Q Q D I V C T V K A H A N D L Y 220
33631 221 I G F K C P S N Y S V E P H D C F V S A 240
33632 241 F N L S G K N E N L E N K L K L T N I I Y 260
33633 261 M D H Y N N T F Y S R L P S L I S D N W 280
33634 281 K F F C V C S K D N E K K L V F T V E A Y 300
33635 301 S I S S S N T K L A S R D N T Y Q D Y I 320
33636 321 S N S S F L T L S S Y C A F I T F I I T 340
33637 341 L S S Y C A F I T F I I T S F L S F I L 360 ND
(b)
Peptide number
Pf38
Specific Binding Activity (%)
2
SS
I
II
Tm
33638 1 M K R W S I I T G I V I I F C I L T C K Y 20
33639 21 G Q V E N K K V D F R T E K G K F V P L Y 40
33640 41 N L V P G D V V E Y S C P Y S L N N D I 60
33641 61 R N M N G V E R E H F D N K K F C F D Y 80
33642 81 I F V G S K L T F L K E Y V R G S Y N V 100
33643 101 V H K E E G N L Y T S Q F S V P P V V L 120
33644 121 T H R N F D C F C Y M E E N N V V V K K 140
33645 141 V L R I H I S N G V L R K I P G C D F N Y 160
33646 161 A D Y K E S T A I T T F S N M S P R R V 180
33647 181 K V C D V Y P K S G D F I S L M C P S D 200
33648 201 Y S I K P D G C F S N V Y V K R Y P N E 220
33649 221 E V K E E D R F N L N R K W D A S K Y N 240
33650 241 V V S I E T V L K M N M I T Q G D K Y S 260
33651 261 I F S K L P D V K D Q V D F T C I C Q S Y 280
33652 281 N D E Q D N L M M N V Y I N N T S Y L T 300 ND
33653 301 N N T R S I G V N K H S F S N S E I F E Y 320
33654 321 R I E R E E I S F A F S S Y L S I T L I 340 ND
33655 341 A F S S Y L S I T L I L L Y L F F L N F 360
(c)
Peptide number
Pf41
Specific Binding Activity (%)
2
SS
I
II
33700 1 M K G V I F C L V V L L W R Q A W V S S Y 20
33701 21 K S H K C D F T K E K Y L L S G E K E V 40
33702 41 S C E I D A N P S D D I T F I C P N K I Y 60
33703 61 D S L C F H T V N I S K N I N Q N K S T Y 80
33704 81 M S I Q D L L Y G S V V Y G N T L F I S P 100 ND
33705 101 Y V R T N T P F Y C F C N L D T V T I Q 120
33706 121 K F L K I N R F L K D D D E L S E A D V Y 140
33707 141 M K H L K G G N V S E A Q A D E Y L N K 160
33708 161 A L N R F K K M K D L S K F F N D Q A D Y 180
33709 181 N T T K L N L P K S L N I P N D I L N Y 200
33710 201 D V Y N S S N N R N D I V V K D E V T N 220
33711 221 K Q I I S K R G I M S V F V R S N N N V Y 240
33712 241 I K G C D F G N N N K N Y F S H P I S V 260
33713 261 A G K V N N K V C K I Q G K P G E L V G Y 280
33714 281 F K C A F E E N G K V E P P N C F D Q V Y 300
33715 301 L H K N K V T D L K T L I P G Y A S Y T 320
33716 321 N K H S S K Y P Y Y L K I P H F V N E Q 340
33717 341 Y T I Q C K C K S N N S Q N E Y T F E L 360 ND
33718 361 F E L D I Q P G E S E V V L N S F K T S Y 380
(d)
Peptide number
Pf12
Specific Binding Activity (%)
2
33625 101 V I G S S M F M R R S L T P N K I N E V Y 120
36090 - M R I S R K G S P T M S V N F E L N V I Y -
33633 261 M D H Y N N T F Y S R L P S L I S D N W 280
36091 - W N D N I M D P S Y T R F Y N S L L S H -
Peptide number
Pf38
Specific Binding Activity (%)
2
33645 141 V L R I H I S N G V L R K I P G C D F N Y 160
36092 - G V R P H F I K D I S N N G I V L C L R Y -
33648 201 Y S I K P D G C F S N V Y V K R Y P N E 220
36093 - S V Y Y K S P F K P V D E G N N R C I Y -
Peptide number
Pf41
Specific Binding Activity (%)
2
33708 161 A L N R F K K M K D L S K F F N D Q A D Y 180
36094 - D R Q L F A A F K K M S N N D F L D K K Y -

Table 1
Dissociation constants (K_d), Hill coefficients (nH) and binding sites per cell (BSC) for HABPs identified in *Pf*12, *Pf*38 and *Pf*41.

Protein	Peptide	K_d (nM)[a]	nH[a]	BSC[a]
*Pf*12	33633	1000	1.0	23690
*Pf*38	33648	550	0.6	24560
*Pf*41	33708	850	1.2	22645
	33709	750	1.2	84322
	33713	350	1.2	24092
	33715	550	1.1	40153

[a] All standard deviations were below 9%.

Table 2
Effect of the enzymatic treatment on HABPs' binding to erythrocytes.

Protein	Peptide	Neuraminidase[a,b]	Chymotrypsin[a,b]	Trypsin[a,b]
*Pf*12	33625	48	30	23
	33633	0	18	23
*Pf*38	33645	0	0	38
	33648	68	0	0
*Pf*41	33708	62	13	47
	33709	14	190	55
	33713	196	293	154
	33715	50	145	177

[a] Binding percentage to enzyme-treated erythrocytes.
[b] All standard deviations were below 7%.

3. Results

3.1. Pf12, Pf38 and Pf41 peptides showing high specific binding activity to erythrocytes

A total of eight HABPs were identified in *Pf*12, *Pf*38 and *Pf*41. In *Pf*12, HABP 33625 ^{101}VIGSSMFMRRSLTPNKINEV^{120} was located towards the N-terminal region in the Cys-rich domain I while HABP 33633 ^{261}MDHYNNTFYSRLPSLISDNW^{280} was situated at the C-terminal region of the Cys-rich domain II (Fig. 2a). The *Pf*38 protein presented also two HABPs: 33645 ^{141}VLRIHISNGVLRKIPGCDFN^{160} and 33648 ^{201}YSIKPDGCFSNVYVKRYPNE^{220}, both located in the Cys-rich domain II (Fig. 2b). Finally, *Pf*41 contained four HABPs (Fig. 2c): HABP 33708 ^{161}ALNRFKKMKDLSKFFNDQAD^{180}, 33709 ^{181}NTTKLNLPKSLNIPNDILNY^{200}, 33713 ^{261}AGKVNNKVCKIQGKPG-ELVG^{280} and 33715 ^{301}LHKNKVTDLKTLIPGYASYT^{320}. The first two HABPs were located in the protein's central region outside both Cys-rich domains, whereas the other two HABPs were situated towards the C-terminus region inside the Cys-rich domain II (Fig. 2c).

Binding assays to erythrocytes carried out with scrambled HABPs (*i.e.* peptides having the same amino acid composition but with different sequence) demonstrated that HABPs' binding depended exclusively of their amino acid sequence and therefore possibly on their structural configuration, since their specific binding activity diminished when their sequences were altered (scrambled sequence-HABP analogues had <2% specific binding activity) (Fig. 2d).

3.2. Dissociation constants of the binding complex

Binding constants of each HABP were determined in saturation assays (Fig. 3). All HABPs' specific bindings were saturable and presented nanomolar dissociation constants (K_d). Hill coefficients were >1 for most high specific binding peptides and the number of receptors per cell ranged between 20,000 and 85,000 (Table 1).

3.3. HABP binding to erythrocytes is differentially affected by the enzymatic treatments

The nature of the erythrocyte surface receptor(s) of each identified HABPs was partially characterized by testing HABPs' binding to neuraminidase, chymotrypsin or trypsin treated erythrocytes. Each HABP's binding was differentially affected by each enzymatic treatment, suggesting interactions with glycoproteic and/or non-glycoproteic receptors (Table 2).

3.4. Erythrocyte membrane receptors for Pf12, Pf38 and Pf41 HABPs

Some radiolabeled HABPs were cross-linked to erythrocytes in order to determine the molecular weight of their possible erythrocyte surface receptor(s). As indicated in the autoradiogram shown in Fig. 4, *Pf*12 HABP 33625, *Pf*38 HABP 33648 and *Pf*48 HABPs 33713 and 33715 recognized bands with molecular weights ranging between 28 and 95 kDa. Furthermore, such recognition was inhibited in the presence of each HABPs' corresponding unlabeled peptide (see even lanes in Fig. 4a and b), thus indicating specificity of HABPs binding to erythrocyte membrane proteins.

3.5. HABPs inhibit merozoite invasion of erythrocytes in vitro

The possible role of *Pf*12, *Pf*38 and *Pf*41 HABPs during merozoite's invasion to erythrocytes was evaluated *in vitro* in invasion inhibition assays. The results showed that all HABPs inhibited moderately *P. falciparum* invasion of erythrocytes, with standard deviations below 5% being obtained in all assays (Table 3), whereas random-sequence peptides having the same amino acid composition as *Pf*12, *Pf*38 and *Pf*41 HABPs did not inhibit invasion. Mixtures containing HABPs from each of these three proteins exhibited significant invasion inhibition ability (Table 3).

3.6. HABPs secondary structure

Circular dichroism (CD) spectra (Fig. 5) obtained for all HABPs derived from the Cys_6 proteins assessed in this study, with their corresponding deconvolution using SELCON, CONTINLL and CDSSTR programs; [43–45] show β-turn and α-helix features as being the main structural characteristics of these HABPs.

4. Discussion

The *P. falciparum* Cys_6 protein family comprises 10 proteins expressed by asexual and sexual development stages [5,13,14]. Proteins belonging to this family have a characteristic pattern of six conserved cysteine residues defining two or more notably conserved domains (Fig. 1a and b) [5]. In *P. falciparum*, the GPI-anchored proteins *Pf*12 and *Pf*38, and the non-covalently associated *Pf*41 surface protein have been detected in detergent-resistant lipid raft domains (Fig. 1c) and have been implicated in merozoite invasion to erythrocytes [13,46]. The structural configuration of *Pf*12 and *Pf*41

Fig. 2. Binding profiles of the synthetic peptides derived from *Plasmodium falciparum* Cys_6 family proteins *Pf*12 (a), *Pf*38 (b), *Pf*41 (c) and some random-sequence analogues of *Pf*12, *Pf*38 and *Pf*41 HABPs (d). Each peptide's binding activity is indicated by the length of horizontal black bar in front of their corresponding amino acid sequence. The structure of each protein is represented by the vertical bar at the left, showing domain I in light gray, domain II in dark gray; the signal peptide is marked by diagonal lines while transmembranal domains are indicated by horizontal lines, while segments corresponding to HABPs are filled in black. Cysteine residues forming part of each Cys-rich domain are encircled within each protein's sequence. Scrambled HABP analogues did not present a high binding activity to erythrocytes in contrast to their corresponding HABPs.

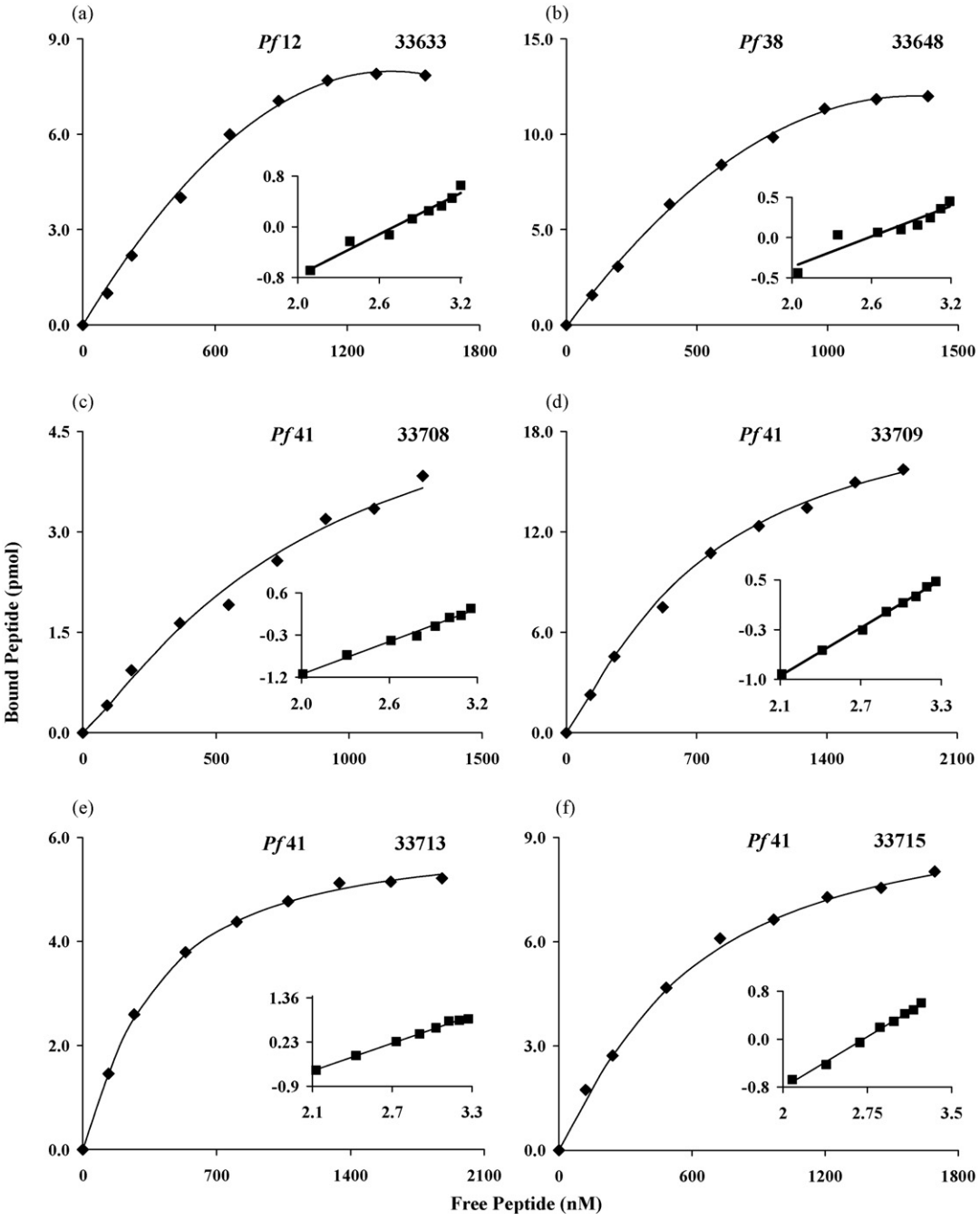

Fig. 3. Saturation assays for Cys_6 family proteins *Pf*12 (a), *Pf*38 (b), *Pf*41 (c–f) HABPs. The curve represents HABP's specific binding to erythrocytes. In the Hill graph (inside), the abscissa is log *F* and the ordinate log (*B*/Bmax-*B*), being *F* the amount of free peptide, *B* the amount of bound peptide and Bmax the maximum amount of bound peptide.

shows the presence of six disulfide bonds inside two Cysteine-rich domains (Figs. 1 and 2). In the case of *Pf*38, five possible disulfide bridges are formed, two between cysteines inside domain I and three between Cys 157–183, 197–278 and 208–276 located inside domain II [5].

In this study, the *Pf*12, *Pf*38 and *Pf*41 proteins were finely mapped by synthesizing their complete amino acid sequences as 20-mer peptides and testing the binding ability of these peptides through a robust and highly specific binding assay suitable for identifying peptides binding specifically and with high activity to human erythrocytes. Once these HABPs were identified, their binding interactions were characterized in saturation, enzymatic treatment and cross-linking assays, their main secondary structural features were determined by CD and their biological relevance was examined *in vitro* by performing invasion inhibition assays. The results revealed the presence of HABPs 33625 and 33633 in *Pf*12, HABPs 33645 and 33648 in *Pf*38 and HABPs 33708, 33709, 33713 and 33715 in *Pf*41.

The results show that both HABPs derived from *Pf*12 are located within Cys-rich domains of this protein. HABP 33625 is located between Cys 4 and 5 (81–136) of domain I, while HABP 33633 is flanked by Cys 4′ and 5′ (236–284) of domain II (Figs. 1a and 2a). Interestingly, *Pf*38 HABP 33648 and *Pf*41 HABP 33715 are also located in domain II (Fig. 2b and c) inside the same loop where *Pf*12 HABP 33633 is located, which suggests that the two loops formed between the aforementioned Cys residues might be directly involved in bimolecular interactions established between these three Cys_6 family members and erythrocyte receptors during parasite invasion to erythrocytes. Accordingly, peptide 33704, which

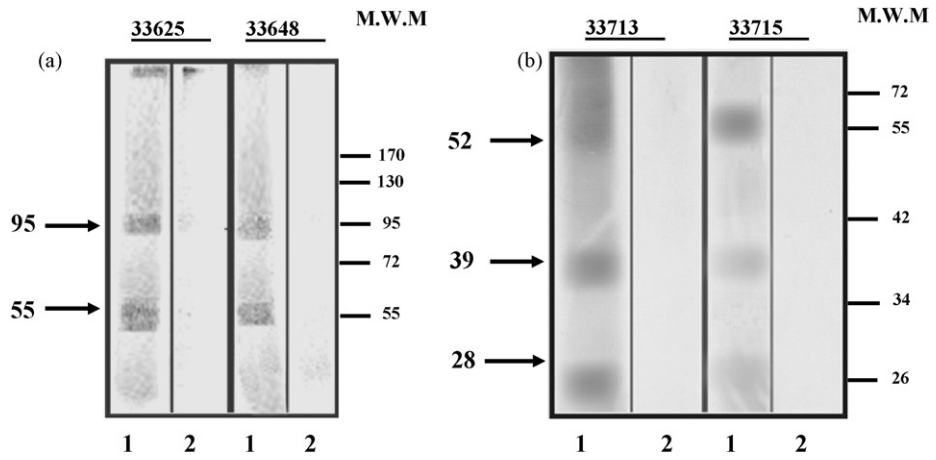

Fig. 4. Autoradiogram of cross-linking assays for *Pf*12 *Pf*38, *Pf*41 HABPs. Erythrocyte membrane proteins were cross-linked to the radiolabeled HABPs. (a) *Pf*12 33625 and *Pf*38 33648, (b) *Pf*41 33713 and 33715. In all autoradiograms, lane 1 corresponds to cross-linked proteins in the absence of unlabeled peptide and lane 2 to cross-linking in the presence of unlabeled peptide. The apparent molecular weight of the identified proteins is shown on the left, while the migration of reference molecular weight markers (MWM) is shown on the right.

is located inside the same region as *Pf*12 HABP 33625 (between Cys 4 and 5 of domain I), could be also involved in *Pf*41 binding to erythrocytes, but unfortunately, such involvement could not been confirmed due this peptide's low solubility under the experimental conditions followed in the binding assays here presented (Fig. 2c).

HABPs 33708 and 33709 derived from *Pf*41 were identified inside the region connecting the two domains of this protein, which in this protein compromises a larger region than in *Pf*12, and therefore is more accessible and could more easily participate in *Pf*41 binding to erythrocytes (Fig. 2c). *Pf*38 HABPs 33645 and 33648 were both located inside domain II, which contains the same disulfide bridges predicted for the other Cys_6 proteins (Fig. 2b) [5], while *Pf*41 HABP 33713 is located within the same domain II region containing Cys 2′ (Fig. 2c).

The arrangement of *Pf*12, *Pf*38 and *Pf*41 HABPs within domain II is illustrated in the Clustal W alignment [47] shown in Fig. 6. The conspicuous localization of these HABPs within the loops flanked by the conserved Cys residues 4′ and 5′ suggests a possible role of this region in protein–protein interactions. This finding gives additional supports to our suggestion of the existence of a binding domain in the Cys_6 protein family mediating interactions with erythrocyte receptors, same as it has been described for several *P. falciparum*

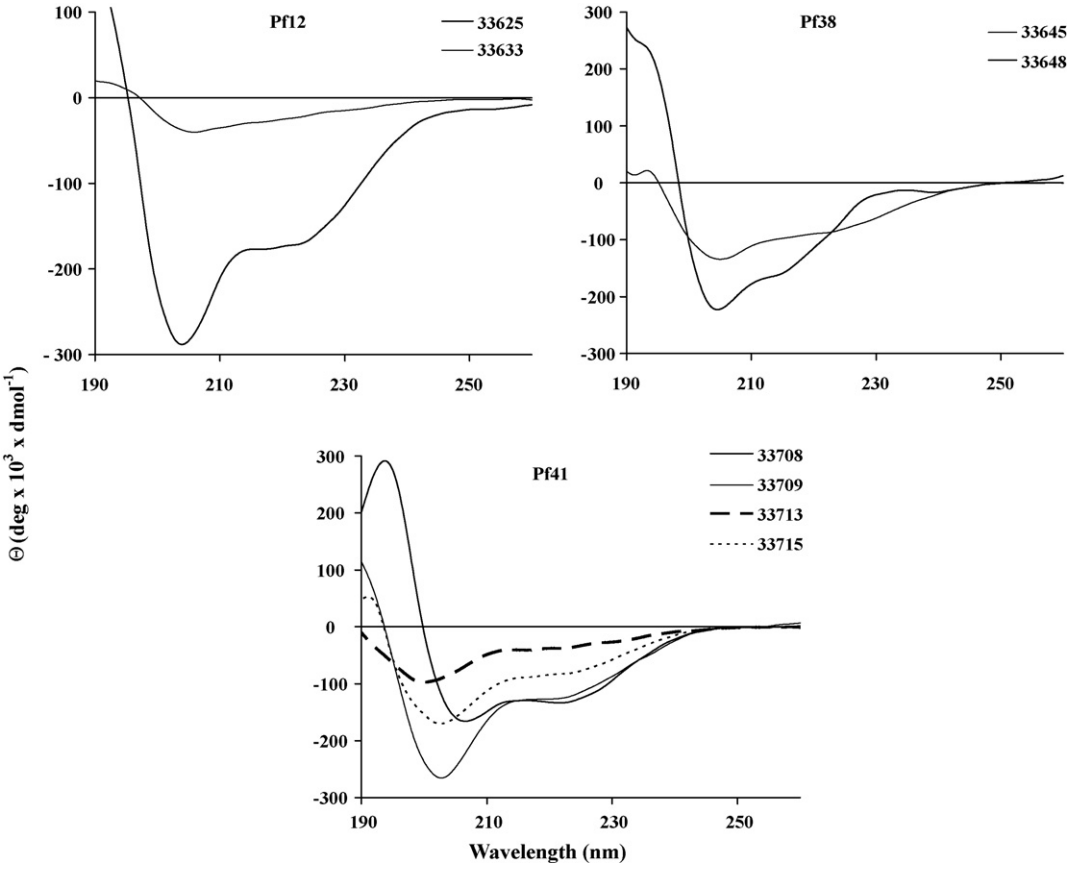

Fig. 5. Circular dichroism of HABPs identified in the *P. falciparum* Cys_6 family proteins *Pf*12, *Pf*38 and *Pf*41 HABP. All spectra were obtained in 30% TFE.

Table 3
In vitro inhibition of merozoite invasion to erythrocytes by HABPs derived from *P. falciparum* Cys_6 family proteins.

Protein	Peptide	Invasion inhibition (%)[a,b,c]
*Pf*12	33625	23
	33633	18
*Pf*38	33645	33
	33648	20
*Pf*41	33708	22
	33709	24
	33713	**51**
	33715	16
Scrambled peptides	36090	0
	36091	8
	36093	3
	36094	3
Mixtures	33633, 33648, 33715	**41**
	33625, 33645, 33708	**54**
	33625, 33648, 33709	**37**
Control (EGTA 50 mM)		**55**
Chloroquine		**100**

[a] All standard deviations were below 5%.
[b] Invasion inhibition values above or equal to 40% are highlighted in bold types.
[c] Mixtures were prepared in a 1:1:1 ratio.

proteins containing other types of Cys-rich domains such as the Duffy-binding like (DBL) motif [26,48,49].

According to the results of saturation assays, Cys_6 HABPs bound specifically and with high affinity to erythrocyte receptors as indicated by their nanomolar dissociation constants. Additionally, binding of Cys_6 HABPs showed Hill coefficients values greater than one, except for *Pf*38 HABP 33648 (Fig. 3 and Table 1) [17,18,38,39].

The possible nature of the erythrocyte membrane receptors of *Pf*12, *Pf*38 and *Pf*41 HABPs was studied in binding assays with enzyme-treated erythrocytes and cross-linking assays. According to the results of enzyme-treatment assays, specific binding of *Pf*12 HABPs 33625 and 33633, as well as of *Pf*38 HABP 33645 diminished (50–80%) when erythrocytes were treated with neuraminidase, chymotrypsin or trypsin (Table 2). Such binding pattern suggests the interaction of these HABPs with glycosylated and/or non-glycosylated proteic receptor(s). In contrast, binding of *Pf*38 HABP 33648 was totally suppressed by treating erythrocytes with chymotrypsin and trypsin, suggesting binding to erythrocyte surface receptors of proteic nature [50].

Regarding *Pf*41 HABPs, the majority of HABPs presented an increased binding ability to chymotrypsin-treated erythrocytes (except for peptide 33708 whose binding was diminished, possibly due to its interaction with membrane proteins such as band 3 protein or in a minor proportion with sugar-containing receptors), suggesting their interaction with cryptic receptors exposed by the enzymatic digestion of erythrocyte membranes. The presence of cryptic epitopes was especially notable for HABP 33713, whose binding ability increased with all the enzymatic treatments being applied. On the contrary, HABP 33709 binding was sialic acid-dependent, as demonstrated by the drastic reduction of its binding ability when erythrocyte membranes were treated with either neuraminidase (almost a 90% reduction) or trypsin (~45% reduction) (Table 2). These results point out to sialic acid-containing receptors such as glycophorin A and C for this HABP [50]. Finally, HABP 33715 binding was only sensitive to treatment with neuraminidase, indicating binding to sialic acid-containing receptors such as glycoproteins or the putative "Y" receptor [50].

Autoradiograms of *Pf*12 HABP 33625 and *Pf*38 HABP 33648 obtained from cross-linking assays indicate the interaction of these peptides with proteins of 95 and 55 kDa. These molecular weights, together with the results of enzymatic treatment assays, point towards proteins such as band 3 and glycophorin A [50], respectively, as the erythrocyte membrane receptors for these HABPs (Fig. 4a). In contrast, the *Pf*41 HABPs 33713 and 33715 recognized bands of around 52, 39 and 28 kDa (Fig. 4b), suggesting the interaction of these HABPs with members of the glycophorin protein family such as glycophorin A (52 kDa), B (28 kDa) and C (37 kDa), which agrees with the sialic acid-dependent susceptible binding evidenced by treating erythrocytes with neuraminidase and trypsin [50]. It is worth noting that even though the results of cross-linking and enzymatic treatment assays strongly suggest the recognition of these erythrocyte surface molecules by *Pf*12, *Pf*38 and *Pf*41 HABPs, further assays are needed in order to elucidate the precise nature of each HABPs' receptor.

Additionally, differences in binding and invasion inhibition ability between HABPs and scrambled peptides were analyzed by comparing their respective binding medians (2.775 and 0.725, respectively) and medians of invasion inhibition (28.875 and 3.5, respectively) by applying a Mann–Whitney test. This statistical analysis was performed using STATA software [51] setting a significance level of 0.05. Significant differences were found in both metrics (binding: Mann–Whitney rank sum test, $z = 2.737$, $p = 0.0062$; inhibition: Mann–Whitney rank sum test, $z = 2.722$, $p = 0.0065$), indicating the statistical relevance of HABPs' binding ability and invasion inhibition ability compared to control peptides (*i.e.* scrambled peptides derived from these same HABPs).

Regarding CD assays, *Pf*12 HABP 33625 presented two minima at 203 and 222 nm slightly differing with the characteristic double minima at 208 and 222 nm of α-helical configurations, which are probably indicative of the presence of β-turn or random coil features. On the other hand, HABP 33633 had only a minimum at 204 nm, indicating the predominant presence of β-turn or random coil features in its structure. By the same way, *Pf*38 HABPs 33645 and 33648 displayed a similar configuration to that of HABP 33625 (Fig. 5), while *Pf*41 HABPs 33708, 33709, 33713 and 33715 displayed α-helical structure features, with a slight displacement of their minima possibly due to the presence of other structural features.An analysis of these spectra using SELCON3, CONTINLL and CDSSTR programs confirmed the above detailed observations, showing a 15–30% α-helical content in *Pf*12 and *Pf*38 HABPs, and mainly β-

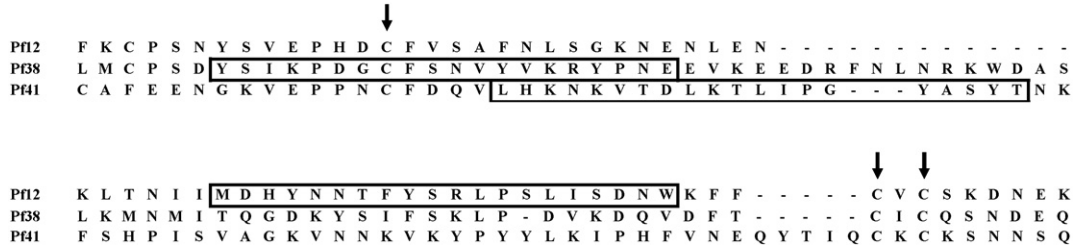

Fig. 6. Alignment of *Pf*12, *Pf*38 and *Pf*41 Cys-rich domains showing the conserved cysteine residue pattern typical of the Cys_6 protein family. HABPs 33633 (*Pf*12), 33648 (*Pf*38) and 33715 (*Pf*41) are enclosed in black boxes.

turn elements on all peptide structures. Conversely, *Pf*41 HABPs presented a more significant percentage of α-helix configurations (45–69%). Bearing in mind that *Pf*12 and *Pf*38 are GPI-anchored proteins, in contrast to *Pf*41 which is non-covalently associated to other membrane proteins; these results are in complete agreement with the functional, structural and immunological compartmentalization of *P. falciparum* invasion proteins proposed by Reyes et al., highlighting the importance of the relationship between the structure and biological activity of each HABP for interacting with the immune system's HLA molecules [52]. Furthermore, these results are in complete agreement with the structural features predicted by Gerloff et al. for Cys_6 family protein members [5].

According to the results of invasion inhibition assays, all HABPs had a low to moderate invasion inhibition ability (28–51%), being *Pf*41 HABP 33713 the one showing the highest invasion inhibition percentage (51%) at 200 μM. On the contrary, merozoite invasion was not inhibited by scrambled peptides having the same amino acid composition of these HABPs, thus indicating the specificity of all performed assays. The moderate ability of HABPs to inhibit erythrocyte invasion suggest that *Pf*12, *Pf*38 and *Pf*41 are acting in association with other merozoite membrane proteins (possibly other DRM-associated proteins) and are probably used by *P. falciparum* parasites as an alternative invasion pathway to evade the host's immune system response [13]. This observation can be validated by the invasion inhibition ability of the three *Pf*12, *Pf*38 and *Pf*41 HABP mixtures (37–54%) tested in this study, which was more significant than the inhibition reached with each HABP individually. These findings lead us to suggest that the *P. falciparum* Cys_6 proteins included in this study are possibly acting as *P. falciparum* ligands during erythrocyte invasion and hence support the inclusion of *Pf*12, *Pf*38 and *Pf*41 Cys_6 family members as potential antimalarial vaccine candidates.

In this work, we have identified and partially characterized sequences showing high specific binding activity to erythrocytes in the multi-stage Cys_6 family members *Pf*12, *Pf*38 and *Pf*41, which lead us to suggest the presence of a conserved erythrocyte binding region in Cys_6 proteins. The results indicate that HABPs identified on these merozoite membrane proteins are interesting targets for immunogenicity studies, as it has been reported that modifications done to non-immunogenic conserved HABPs can induced a protective immune response against *P. falciparum* challenge in *Aotus* monkeys [16,23,30,53]. These HABPs are therefore postulated as potential candidates to be included in the design of a new fully effective, multiepitope, subunit-based, multi-stage, synthetic antimalarial vaccine currently being developed at our Institute.

Acknowledgements

This study was supported by COLCIENCIAS, contract RC-2008. We would like to thank Nora Martinez for translating the manuscript.

References

[1] Snow RW, Guerra CA, Noor AM, Myint HY, Hay SI. The global distribution of clinical episodes of *Plasmodium falciparum* malaria. Nature 2005;434(March (7030)):214–7.
[2] Gaur D, Mayer DC, Miller LH. Parasite ligand-host receptor interactions during invasion of erythrocytes by *Plasmodium* merozoites. Int J Parasitol 2004;34(December (13–14)):1413–29.
[3] Cowman AF, Baldi DL, Duraisingh M, Healer J, Mills KE, O'Donnell RA, et al. Functional analysis of *Plasmodium falciparum* merozoite antigens: implications for erythrocyte invasion and vaccine development. Philos Trans R Soc Lond B Biol Sci 2002;357(January (1417)):25–33.
[4] Cowman AF, Crabb BS. The *Plasmodium falciparum* genome—a blueprint for erythrocyte invasion. Science 2002;298(October (5591)):126–8.
[5] Gerloff DL, Creasey A, Maslau S, Carter R. Structural models for the protein family characterized by gamete surface protein Pfs230 of *Plasmodium falciparum*. Proc Natl Acad Sci USA 2005;102(September (38)):13598–603.
[6] Healer J, McGuinness D, Carter R, Riley E. Transmission-blocking immunity to *Plasmodium falciparum* in malaria-immune individuals is associated with antibodies to the gamete surface protein Pfs230. Parasitology 1999;119(November (Pt 5)):425–33.
[7] Sanders PR, Cantin GT, Greenbaum DC, Gilson PR, Nebl T, Moritz RL, et al. Identification of protein complexes in detergent-resistant membranes of *Plasmodium falciparum* schizonts. Mol Biochem Parasitol 2007;154(August (2)):148–57.
[8] Thompson J, Janse CJ, Waters AP. Comparative genomics in *Plasmodium*: a tool for the identification of genes and functional analysis. Mol Biochem Parasitol 2001;118(December (2)):147–54.
[9] Templeton TJ, Kaslow DC. Identification of additional members define a *Plasmodium falciparum* gene superfamily which includes Pfs48/45 and Pfs230. Mol Biochem Parasitol 1999;101(June (1–2)):223–7.
[10] Gardner MJ, Hall N, Fung E, White O, Berriman M, Hyman RW, et al. Genome sequence of the human malaria parasite *Plasmodium falciparum*. Nature 2002;419(October (6906)):498–511.
[11] van Schaijk BC, van Dijk MR, van de Vegte-Bolmer M, van Gemert GJ, van Dooren MW, Eksi S, et al. Pfs47, paralog of the male fertility factor Pfs48/45, is a female specific surface protein in *Plasmodium falciparum*. Mol Biochem Parasitol 2006;149(October (2)):216–22.
[12] Ishino T, Chinzei Y, Yuda M. Two proteins with 6-cys motifs are required for malarial parasites to commit to infection of the hepatocyte. Mol Microbiol 2005;58(December (5)):1264–75.
[13] Sanders PR, Gilson PR, Cantin GT, Greenbaum DC, Nebl T, Carucci DJ, et al. Distinct protein classes including novel merozoite surface antigens in Raft-like membranes of *Plasmodium falciparum*. J Biol Chem 2005;280(December (48)):40169–76.
[14] Gilson PR, Nebl T, Vukcevic D, Moritz RL, Sargeant T, Speed TP, et al. Identification and stoichiometry of glycosylphosphatidylinositol-anchored membrane proteins of the human malaria parasite *Plasmodium falciparum*. Mol Cell Proteomics 2006;5(July (7)):1286–99.
[15] Elliott JF, Albrecht GR, Gilladoga A, Handunnetti SM, Neequaye J, Lallinger G, et al. Genes for *Plasmodium falciparum* surface antigens cloned by expression in COS cells. Proc Natl Acad Sci USA 1990;87(August (16)):6363–7.
[16] Patarroyo ME, Patarroyo MA. Emerging rules for subunit-based, multiantigenic, multistage chemically synthesized vaccines. Acc Chem Res 2008;41(March (3)):377–86.
[17] Curtidor H, Urquiza M, Suarez JE, Rodriguez LE, Ocampo M, Puentes A, et al. *Plasmodium falciparum* acid basic repeat antigen (ABRA) peptides: erythrocyte binding and biological activity. Vaccine 2001;19(August (31)): 4496–504.
[18] Pinzon CG, Curtidor H, Bermudez A, Forero M, Vanegas M, Rodriguez J, et al. Studies of *Plasmodium falciparum* rhoptry-associated membrane antigen (RAMA) protein peptides specifically binding to human RBC. Vaccine 2008;26(February (6)):853–62.
[19] Rodriguez LE, Urquiza M, Ocampo M, Suarez J, Curtidor H, Guzman F, et al. *Plasmodium falciparum* EBA-175 kDa protein peptides which bind to human red blood cells. Parasitology 2000;120(March (Pt 3)):225–35.
[20] Urquiza M, Rodriguez LE, Suarez JE, Guzman F, Ocampo M, Curtidor H, et al. Identification of *Plasmodium falciparum* MSP-1 peptides able to bind to human red blood cells. Parasite Immunol 1996;18(October (10)):515–26.
[21] Torres MH, Salazar LM, Vanegas M, Guzman F, Rodriguez R, Silva Y, et al. Modified merozoite surface protein-1 peptides with short alpha helical regions are associated with inducing protection against malaria. Eur J Biochem 2003;270(October (19)):3946–52.
[22] Cifuentes G, Guzman F, Alba MP, Salazar LM, Patarroyo ME. Analysis of a *Plasmodium falciparum* EBA-175 peptide with high binding capacity to erythrocytes and their analogues using 1H NMR. J Struct Biol 2003;141(February (2)):115–21.
[23] Cubillos M, Salazar LM, Torres L, Patarroyo ME. Protection against experimental *P falciparum* malaria is associated with short AMA-1 peptide analogue alpha-helical structures. Biochimie 2002;84(December (12)):1181–8.
[24] Patarroyo ME, Cifuentes G, Rodriguez R. Structural characterisation of sporozoite components for a multistage, multi-epitope, anti-malarial vaccine. Int J Biochem Cell Biol 2008;40(3):543–57.
[25] Tossavainen H, Pihlajamaa T, Huttunen TK, Raulo E, Rauvala H, Permi P, et al. The layered fold of the TSR domain of *P. falciparum* TRAP contains a heparin binding site. Protein Sci 2006;15(July (7)):1760–8.
[26] Tolia NH, Enemark EJ, Sim BK, Joshua-Tor L. Structural basis for the EBA-175 erythrocyte invasion pathway of the malaria parasite *Plasmodium falciparum*. Cell 2005;122(July (2)):183–93.
[27] Pizarro JC, Chitarra V, Verger D, Holm I, Petres S, Dartevelle S, et al. Crystal structure of a Fab complex formed with PfMSP1-19, the C-terminal fragment of merozoite surface protein 1 from *Plasmodium falciparum*: a malaria vaccine candidate. J Mol Biol 2003;328(May (5)):1091–103.
[28] Feng ZP, Keizer DW, Stevenson RA, Yao S, Babon JJ, Murphy VJ, et al. Structure and inter-domain interactions of domain II from the blood-stage malarial protein, apical membrane antigen 1. J Mol Biol 2005;350(July (4)):641–56.
[29] Lopez R, Curtidor H, Urquiza M, Garcia J, Puentes A, Suarez J, et al. *Plasmodium falciparum*: binding studies of peptide derived from the sporozoite surface protein 2 to Hep G2 cells. J Pept Res 2001;58(October (4)):285–92.
[30] Bermudez A, Cifuentes G, Guzman F, Salazar LM, Patarroyo ME. Immunogenicity and protectivity of *Plasmodium falciparum* EBA-175 peptide and its analog is associated with alpha-helical region shortening and displacement. Biol Chem 2003;384(October–November (10–11)):1443–50.
[31] Cifuentes G, Bermudez A, Rodriguez R, Patarroyo MA, Patarroyo ME. Shifting the polarity of some critical residues in malarial peptides' binding to host cells

is a key factor in breaking conserved antigens' code of silence. Med Chem 2008;4(May (3)):278–92.
[32] Rodriguez LE, Curtidor H, Urquiza M, Cifuentes G, Reyes C, Patarroyo ME. Intimate molecular interactions of *P. falciparum* merozoite proteins involved in invasion of red blood cells and their implications for vaccine design. Chem Rev 2008;108(September (9)):3656–705.
[33] Hall N, Pain A, Berriman M, Churcher C, Harris B, Harris D, et al. Sequence of *Plasmodium falciparum* chromosomes 1,3-9 and 13. Nature 2002;419(October (6906)):527–31.
[34] Houghten RA. General method for the rapid solid-phase synthesis of large numbers of peptides: specificity of antigen–antibody interaction at the level of individual amino acids. Proc Natl Acad Sci USA 1985;82(August (15)):5131–5.
[35] Merrifield RB. Solid phase peptide synthesis. I. The synthesis of a tetrapeptide. J Am Chem Soc 1963;85:2149–54.
[36] Tam JP, Heath WF, Merrifield RB. SN 1 and SN 2 mechanisms for the deprotection of synthetic peptides by hydrogen fluoride, Studies to minimize the tyrosine alkylation side reaction. Int J Pept Protein Res 1983;21(January (1)):57–65.
[37] Yamamura HI, Enna SJ, Kuhar MJ. Neurotransmitter Receptor Binding. New York; 1978.
[38] Hulme EC. Receptor–ligand interactions. A practical approach. New York; 1993.
[39] Weiland GA, Molinoff PB. Quantitative analysis of drug-receptor interactions: I. Determination of kinetic and equilibrium properties. Life Sci 1981;29(July (4)):313–30.
[40] Lambros C, Vanderberg JP. Synchronization of *Plasmodium falciparum* erythrocytic stages in culture. J Parasitol 1979;65(June (3)):418–20.
[41] Wyatt CR, Goff W, Davis WC. A flow cytometric method for assessing viability of intraerythrocytic hemoparasites. J Immunol Methods 1991;140(June (1)):23–30.
[42] Compton LA, Johnson Jr WC. Analysis of protein circular dichroism spectra for secondary structure using a simple matrix multiplication. Anal Biochem 1986;155(May (1)):155–67.
[43] Sreerama N, Venyaminov SY, Woody RW. Estimation of the number of alpha-helical and beta-strand segments in proteins using circular dichroism spectroscopy. Protein Sci 1999;8(February (2)):370–80.
[44] Sreerama N, Woody RW. Estimation of protein secondary structure from circular dichroism spectra: comparison of CONTIN, SELCON, and CDSSTR methods with an expanded reference set. Anal Biochem 2000;287(December (2)):252–60.
[45] van Stokkum IH, Spoelder HJ, Bloemendal M, van Grondelle R, Groen FC. Estimation of protein secondary structure and error analysis from circular dichroism spectra. Anal Biochem 1990;191(November (1)):110–8.
[46] Wang L, Mohandas N, Thomas A, Coppel RL. Detection of detergent-resistant membranes in asexual blood-stage parasites of *Plasmodium falciparum*. Mol Biochem Parasitol 2003;130(August (2)):149–53.
[47] Thompson JD, Higgins DG, Gibson TJ. CLUSTAL W: improving the sensitivity of progressive multiple sequence alignment through sequence weighting, position-specific gap penalties and weight matrix choice. Nucleic Acids Res 1994;22(November (22)):4673–80.
[48] Mayor A, Bir N, Sawhney R, Singh S, Pattnaik P, Singh SK, et al. Receptor-binding residues lie in central regions of Duffy-binding-like domains involved in red cell invasion and cytoadherence by malaria parasites. Blood 2005;105(March (6)):2557–63.
[49] Moll K, Chene A, Ribacke U, Kaneko O, Nilsson S, Winter G, et al. A novel DBL-domain of the *P. falciparum* 332 molecule possibly involved in erythrocyte adhesion. PLoS ONE 2007;2(5):e477.
[50] Baum J, Maier AG, Good RT, Simpson KM, Cowman AF. Invasion by *P. falciparum* merozoites suggests a hierarchy of molecular interactions. PLoS Pathog 2005;1(December (4)):e37.
[51] StataCorp. Stata Statistical Software: Release 10. College Station, TX 2007; StataCorp LP.
[52] Reyes C, Patarroyo ME, Vargas LE, Rodriguez LE, Patarroyo MA. Functional, structural, and immunological compartmentalisation of malaria invasive proteins. Biochem Biophys Res Commun 2007;354(March (2)):363–71.
[53] Espejo F, Bermudez A, Torres E, Urquiza M, Rodriguez R, Lopez Y, et al. Shortening and modifying the 1513 MSP-1 peptide's alpha-helical region induces protection against malaria. Biochem Biophys Res Commun 2004;315(March (2)):418–27.